Optimal Shapes of the Cylindrical Pressurized Fuel Tanks

Prof. PhD. Eng. **Marin BICĂ[1],** Assoc. Prof. PhD. Eng. **Mihai ŢĂLU[2,*]**,
Assoc. Prof. PhD. Eng. **Ştefan ŢĂLU[3]**

[1] University of Craiova, Faculty of Mechanics, Department of Applied Mechanics and Civil Engineering, Calea București Street, no. 107, 200512 Craiova, Dolj county, Romania. E-mail: marinbica52@gmail.com

[2] University of Craiova, Faculty of Mechanics, Department of Applied Mechanics and Civil Engineering, Calea București Street, no. 107, 200512 Craiova, Dolj county, Romania. Corresponding author* e-mail: mihai_talu@yahoo.com

[3] Technical University of Cluj-Napoca, The Directorate of Research, Development and Innovation Management (DMCDI), Constantin Daicoviciu Street, no. 15, Cluj-Napoca, 400020, Cluj county, Romania. E-mail: stefan_ta@yahoo.com

§: All authors contributed equally to this work.

Abstract: *In this paper is made a comparative study of state of stress and liniar deformation which appear in a series of pressurized cylindrical tanks with different end caps designed to store the LPG fuel. Initial design data for the tank design are identical, as well as the lateral cylindrical cover. Taking into account the constructive symmetry of the tanks, models with cross sections ¼ for the side cover, with ¼ at the end caps and with section at 1/8 in the case of the tank assembly are used. It was taken into consideration in the calculation of linear deformation and stress, the simultaneous effect of the temperature and corrosion variation, which reduces the thickness of the tank shells with the increase of the exploitation period. Details of the geometry and the materials selected are also discussed. Finally, it was established for the analyzed group of tanks at the end of the operating period, for the extreme working temperatures, which is the most advantageous form of tank with the minimum stress state and linear deformation.*

Keywords: *Automotive industry, corrosion, crash test, industrial engineering design, optimization, pressurized fuel tank, state of effort*

1. Introduction

The optimal design of the pressurized fuel tanks in automotive industry is an important and practical topic which has been explored for decades [1-3]. This is a key to increasing product competitiveness and safety in exploitation through innovative ideas [4, 5].
The cylindrical pressurized fuel tanks are designed using specific rules for the design, construction, inspection, testing and verification according with the major international standards [6-11].
Basic design criteria include information on corrosion, loadings, design methods, thickness, weld joint coefficients and design of welded joints [5]. In addition, there are well established rules for performing calculations for shells, heads, cones, nozzles, flat covers, flanges and tube sheets [5].
In practice, the cylindrical pressurized fuel tanks are generally preferred because of the simple manufacturing problem and make better use of the available storage space [6-11].
Design study for the stress analysis of cylindrical pressurized fuel tanks due to the various loadings involves the study of longitudinal and circumferential stresses and plays an important role in structural optimization and safety of the equipment [4, 5].
Integrated concurrent engineering techniques [12-15] are employed to enrich the design process of the cylindrical pressurized fuel tanks for representing geometry [16-18] and material details with multidimensional visualization techniques [19-31] to find an optimal geometrical solution [32-34] at less cost.

2. Design procedure of the cylindrical pressurized fuel tanks

The cylindrical pressurized fuel tanks has been analyzed considering the following head covers: a) torospheric type; b) ellipsoidal type; c) for low pressure; d) connected with circular arcs; e) flat; and f) with back head covers connected with circular arcs. The design data used are:

- the lateral cover has a diameter of D = 250 mm and length L = 700 mm;
- the tank material is AISI 4340 steel;
- the maximum hydraulic test pressure: p_{max} = 30 bar;
- the working temperature between the limits: T = -30 ^{0}C up to T = 60 ^{0}C;
- the duration of the tank exploitation: n_a = 20 years;
- the corrosion rate of the material: v_c = 0.1 mm/years;

CAD model generation of the cylindrical pressurized fuel tanks with different types of head covers was done in AutoCAD Autodesk 2017 software [35], (as shown in Figures 1 to 6).

Fig. 1. The tank with torospheric head covers

Fig. 2. The tank with ellipsoidal head covers

Fig. 3. The tank with low pressure head covers

Fig. 4. The tank with head covers connected with circular arcs

Fig. 5. The tank with flat head covers

Fig. 6. The tank with back head covers connected with circular arcs

Optimized CAD design of these tanks was imported to SolidWorks 2017 software [36] for analysis with the: Static, Thermal and Design Study modules.
At first, an optimal design of the lateral cover was made, then has been carried out the optimal design of head cover and finally the state of stress and deformation of the whole tank was performed. At the final stage of exploitation the thickness of the cover is minimal due to the corrosion action and appears the biggest solicitations in the pressurized tank.

2.1. The CAD design of the cylindrical lateral cover

The parameterized model used in calculus is a section of ¼ from the initial cover (Figure 7) and the corresponding surfaces to which the constraints and restrictions are applied are shown in Figure 8.

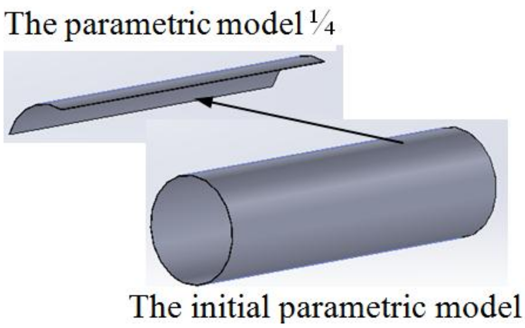

Fig. 7. The parametric model of lateral covers

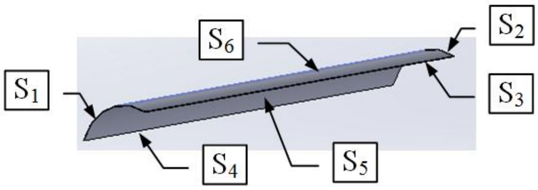

Fig. 8. The ¼ section of lateral head covers where is made the marking of the exterior surfaces

The following parameters were applied as input parameters to the parametric model (Figure 8):
- the maximum pressure p_{max} = 30 N/mm^2 on the inner surface S_5;
- the temperature between the limits: T = -30 ^{0}C to T = 60 ^{0}C on the surface S_6;

- the opposing and equal traction forces of value of F = 36800 N on the surfaces: S_1 and S_2, generated by the action of pressure on the inner surfaces of the head covers;
- the surface symmetry on S_4 and S_5;
- the canceling the displacement of the cover along to the symmetry axis;
- the material of the lateral cover: AISI 4340 steel.

The applied optimization function is intended to achieve a minimum mass. The variable of optimization is the thickness of the cover with limits in range: s = 0.5...3 mm.

The applied restriction of constraint is that the value of Von Mises effort $\sigma_{rez} \leq \sigma_a = 710$ N/mm^2 (σ_a - the admissible value of the traction stress of the material).

Applying the optimization procedure, the obtained values are: the thickness s = 0.59 mm for T = 60 ^{0}C, with the stress value of the $\sigma_{rez.\ max}$= 651.86 N/mm^2 and linear deformation value u_{max} = 0.316 mm. Distributions of linear deformation and state of stress are shown in Figures 9 and 10.

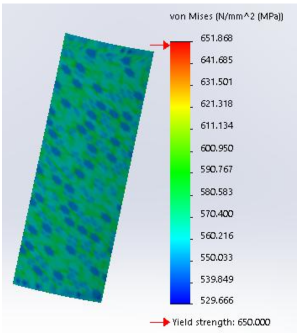

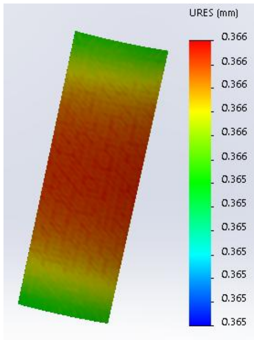

Fig. 9. The graph of Von Mises stress of lateral cover **Fig. 10.** The graph of linear deformation of lateral cover

The optimized thickness of the cover was corrected taking into account: the corrosion phenomenon, the tolerance of negative execution of the sheet laminate and the thinning of the sheet in the embossing process. The formula for calculating the thickness is the following:

$$s_{real} = s_{opt} + \Delta s_c + \Delta s_T + \Delta s_{am} = s_{opt} + v_c \cdot n_a + abs(A_i) + 0.1 \cdot s \quad (1)$$

where: Δs_c, loss of thickness by corrosion; Δs_T, addition of thickness due to the negative tolerance of the laminate sheet; v_c, corrosion velocity of the lateral cover, v_c = 0.1 mm/year; n_a, number of years of exploitation; A_i, lower tolerance of the laminate sheet.

Finally, the minimum value of the sheet thickness is determined as:

$$s_{real\ min} = 0.59 + 0.1 \cdot 20 + abs(-0.6) + 0.1 \cdot 4 = 3.59 \text{ mm} \quad (2)$$

A laminate sheet of AISI 4340 steel with a thickness of s = $4^{+0.25}_{-0.6}$ mm is chosen for analysis.

2.2. The optimized design of the cylindrical pressurized tank with torospheric head covers

The corresponding graphical representations for the optimization of the head cover sectioned to ¼ of the initial model, (as shown in Figure 11 b), and for the parameterized models of tanks sectioned to $^1/_8$ (as shown in Figure 11 c) are given bellow:

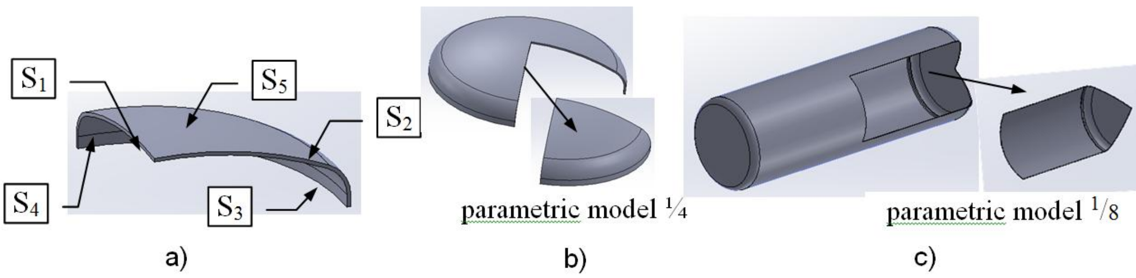

Fig. 11. a) The ¼ section of lateral head cover with the corresponding marking of the exterior surfaces; b) The parametric model at ¼ section of head cover; c) The parametric model at $^1/_8$ section of tank

The sketch and the parametric shaping of the torospheric head cover according to standard DIN 28011 are shown in Figure 12.

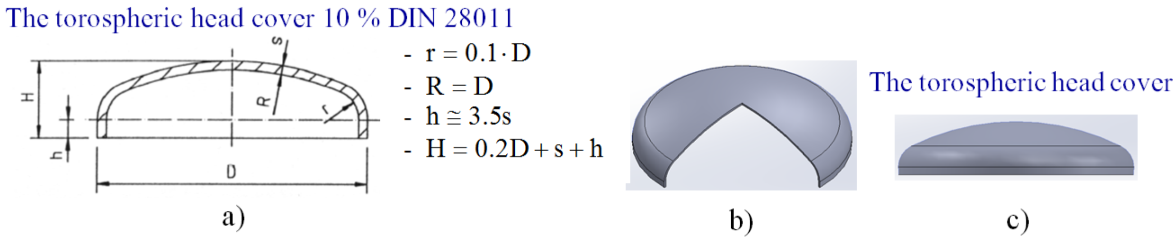

Fig. 12. a) The sketch of torospheric head cover; b) The ¾ section of parametric model of the torospheric head cover; c) The front view of parametric model of the torospheric head cover

According to Fig. 11 a) and for all the following head covers, the following algorithm was applied:

- the maximum pressure p_{max} = 30 N/mm^2 on inner surface S_4;
- the temperature between the limits: T = -30 ^{0}C to T = 60 ^{0}C, on the surface S_5;
- the symmetry on the surfaces: S_1 and S_2;
- the canceling the displacement of the cover along to the symmetry axis.

The cover is optimized to obtain a minimum mass and the effort must be: $\sigma_{rez} \le \sigma_a$ =710 N/mm^2.
The sizes to be optimized are: the cover thickness s = 2...4 mm and the height h = 8...12 mm. The values of dimensions R = D = 250 mm and r = 0.1 · D = 25 mm. The obtained values are: s = 2.38 mm and h = 8.03 mm at T = -30 ^{0}C for the maximum effort $\sigma_{rez.\ max}$ = 652.88 N/mm^2.
The distribution of the stress and linear deformation of the optimal head cover is shown in Figure 13.

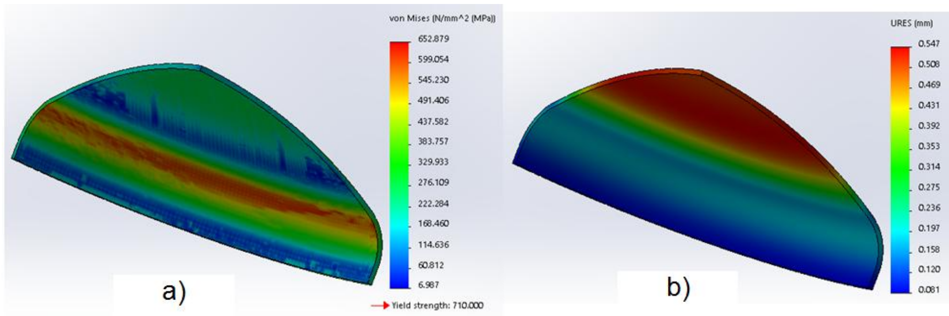

Fig. 13. The graphs for torospheric head cover: a) The Von Mises stress; b) The resultant linear deformation

The correction of the optimal thickness of the cover s is made with the following formula:

$$s_{real\ min} = 2.38 + 0.1 \cdot 20 + abs(-0.6) + 0.1 \cdot 5 = 5.48\ mm \quad (3)$$

A laminate sheet of AISI 4340 steel with a thickness of s = $5.5^{+0.25}_{-0.6}$ mm it was chosen for the manufacturing process. Next dimensions were obtained for the head cover: h ≅ 3.5·s = 20 mm and H = 75.5 mm.
The pressurized tank must resist to n_a = 20 years and the calculation shows that at temperature T = -30 ^{0}C is the maximum stress and at T = 60 ^{0}C the linear resultant deformation is maximal.
For temperature T = -30 ^{0}C the stress and deformation of the tank are shown in Figures 14a and 14b and for T = 60 ^{0}C in Figures 14c and 14d.

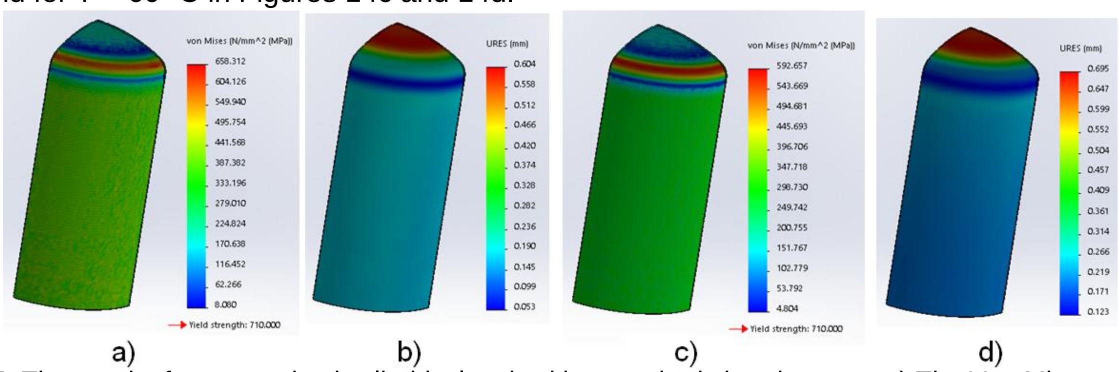

Fig. 14. The graphs for pressurized cylindrical tank with torospheric head covers: a) The Von Mises stress at T = -30 ^{0}C; b) The resultant linear deformation at T = -30 ^{0}C; c) The Von Mises stress at T = 60 ^{0}C; b) The resultant linear deformation at T = 60^{0}C

2.3. The optimized design of the cylindrical tank with ellipsoidal head covers

The sketch and the parametric model of the ellipsoidal cover are shown in Figure 15.

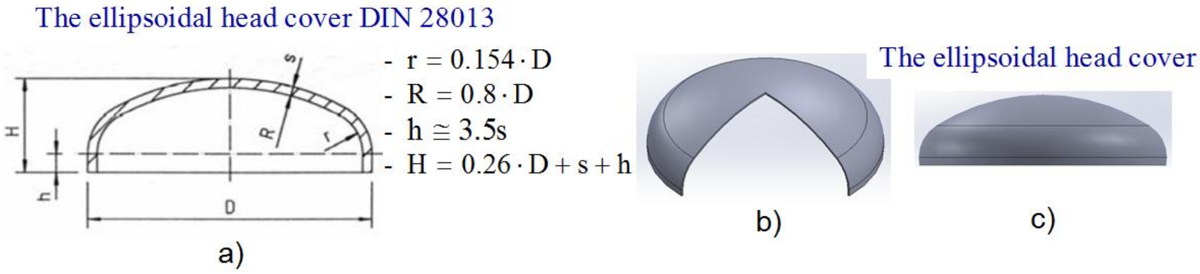

Fig. 15. a) The sketch of ellipsoidal head cover; b) The ¾ section of parametric model of the ellipsoidal head cover; c) The front view of parametric model of the ellipsoidal head cover

The parameters for optimization are: the thickness s = 1...4 mm and the height h = 6...10 mm.
The values of geometric dimensions are: R = 0.8·D = 200 mm and r = 0.154·D = 38.5 mm.
The obtained values are: s = 1.445 mm and h = 6.005 mm with $\sigma_{rez\ max}$ = 594.74 N/mm^2 at T = -30 ^{0}C. The corresponding distribution of stress and linear deformation is shown in Figure 16.

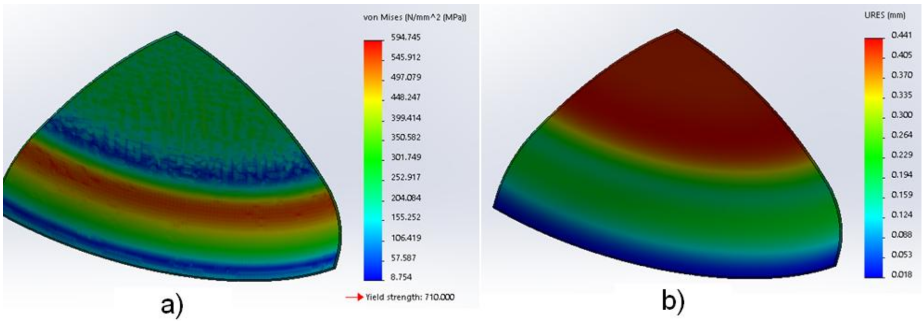

Fig. 16. The graphs for elliptical head cover: a) The Von Mises stress; b) The resultant linear deformation

Finally, the minimum thickness of the cover is:

$$s_{real\ min} = 1.45 + 0.1 \cdot 20 + abs(-0.6) + 0.1 \cdot 4 = 4.45 \text{ mm} \quad (4)$$

A laminate sheet of AISI 4340 steel with a thickness of s = $4.5^{+0.25}_{-0.6}$ mm is chosen.
For the head cover we have the following dimensions: h ≅ 3.5·s = 16 mm and H = 85.5 mm.
The stress and linear deformation of the tank at T = -30 ^{0}C are shown in Figures 17a and 17b, and at T = 60 ^{0}C in Figures 17c and 17d.

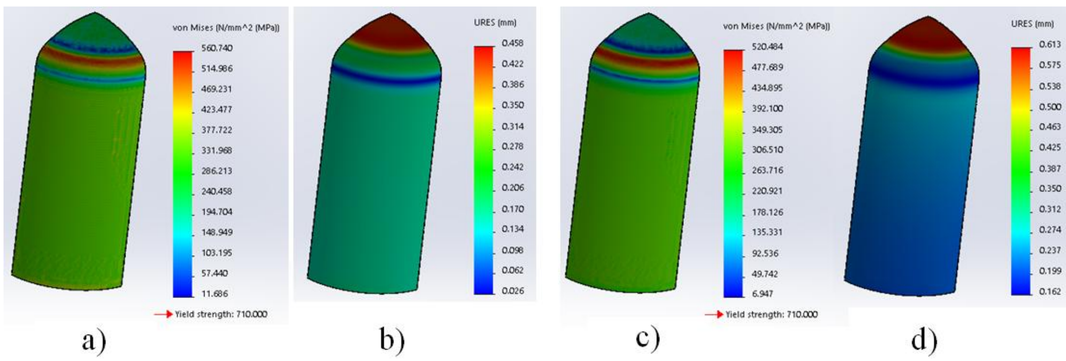

Fig. 17. The graphs for pressurized cylindrical tank with elliptical head covers: a) The Von Mises stress at T = -30 ^{0}C; b) The resultant linear deformation at T = -30 ^{0}C; c) The Von Mises stress at T = 60 ^{0}C; b) The resultant linear deformation at T = 60 ^{0}C

2.4. The optimized design of the cylindrical tank with low pressure head covers

The sketch and the parametric model of the low pressure head cover are shown in Figure 18.
The variables subjected to optimization are: thickness s = 2...5 mm, height h = 12...16 mm and radius r = 15...40 mm. The obtained values are: s = 3.336 mm, h = 12.056 mm, r = 15 mm at T =

-30 ^{0}C with a maximum stress $\sigma_{rez.\ max}$ = 587.68 N/mm^2 and a linear resultant deformation u_{max} = 0.481 mm.

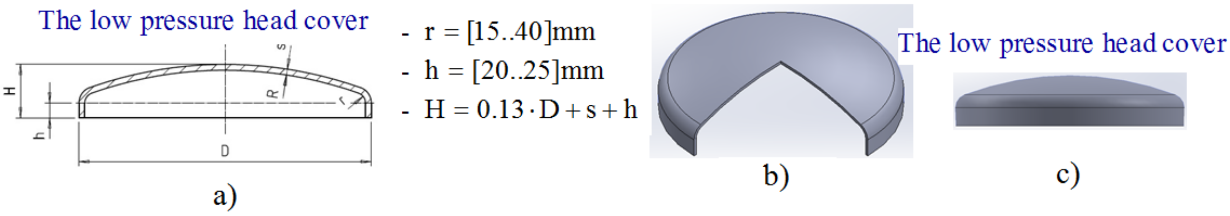

Fig. 18. a) The sketch of the low pressure head cover; b) The ¾ section of parametric model of the low pressure head cover; c) The front view of parametric model of the low pressure head cover

The corresponding graphs of the stress and the state of the resulting linear deformation of the optimal cover head are shown in Figure 19.

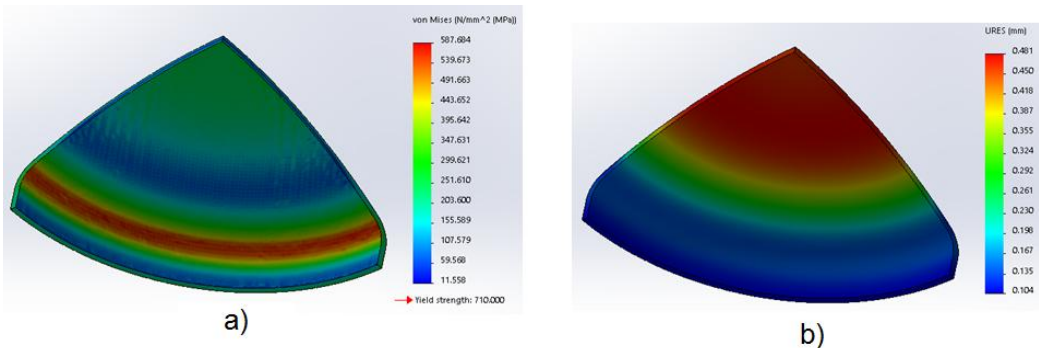

Fig. 19. The graphs for low pressure head cover: a) The Von Mises stress; b) The resultant linear deformation

The minimum real thickness of the cover is:

$$s_{real\ min} = 3.34 + 0.1 \cdot 20 + abs(-0.6) + 0.1 \cdot 6 = 6.54 \text{ mm} \qquad (5)$$

A laminate sheet of AISI 4340 steel with a thickness of s = $6.5^{+0.25}_{-0.6}$ mm was chosen.
For the head cover we have the following dimensions: h ≅ 3.5·s = 22 mm and H = 61 mm.
For temperature T = -30 ^{0}C the stress and deformation of the tank are shown in Figures 20a and 20b and for T = 60^{0}C in Figures 20c and 20d.

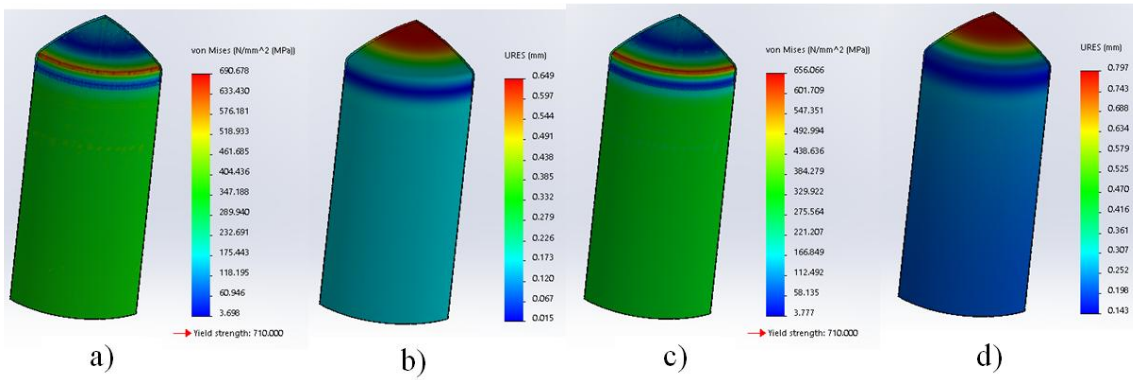

Fig. 20. The graphs for cylindrical tank with low pressure head covers: a) The Von Mises stress at T = -30^{0}C; b) The resultant linear deformation at T = -30 ^{0}C; c) The Von Mises stress at T = 60 ^{0}C; b) The resultant linear deformation at T = 60 ^{0}C;

2.5. The optimized design of the cylindrical tank with caps connected with circular arcs

The sketch and the parametric model of the head cover are shown in Figure 21.
The variables subjected to optimization are: the thickness s = 2...5 mm, the height h = 20...25 mm. and the radius r = 50 mm. The obtained values are: s = 2 mm and h = 12.056 mm at T = -30 ^{0}C, with a maximum stress $\sigma_{rez.\ max}$ = 659.01 N/mm^2 and a linear deformation u_{max} = 0.999 mm.

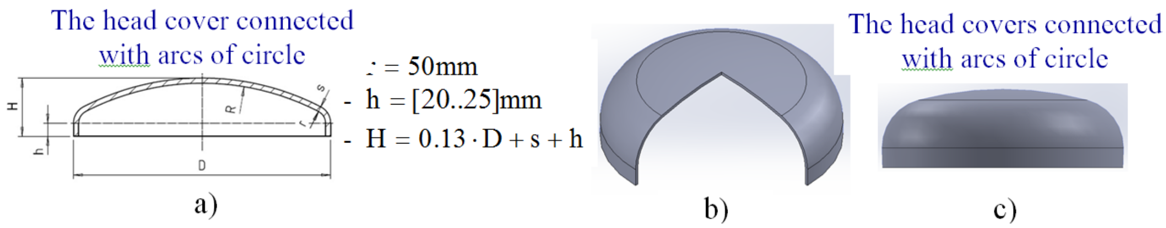

Fig. 21. a) The sketch of head cover connected with circular arcs; b) The ¾ section of model with the head cover connected with circular arcs; c) The front view model of the head cover connected with circular arcs

The corresponding graphs of the stress and the state of the resulting linear deformation of the optimal cover head are shown in Figure 22.

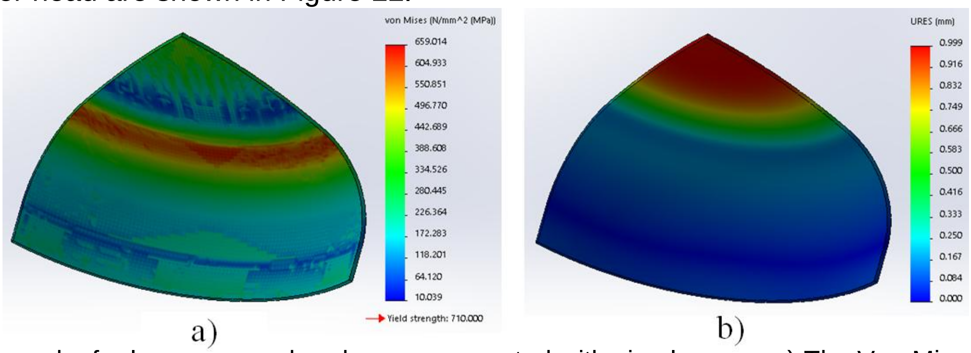

Fig. 22. The graphs for low pressure head cover connected with circular arcs: a) The Von Mises stress; b) The resultant linear deformation.

The minimum thickness of the cover connected with circular arcs is:

$$s_{real\ min} = 2 + 0.1 \cdot 20 + abs(-0.6) + 0.1 \cdot 55 = 5.15 \text{ mm} \qquad (6)$$

A laminate sheet of AISI 4340 steel with a thickness of s = $5.5^{+0.25}_{-0.6}$ mm is chosen. The head cover has the size H = 75 mm. The stress and linear deformation of the tank at T = -30 ^{0}C are shown in Figures 23a and 23b and at T = 60 ^{0}C in Figures 23c and 23d.

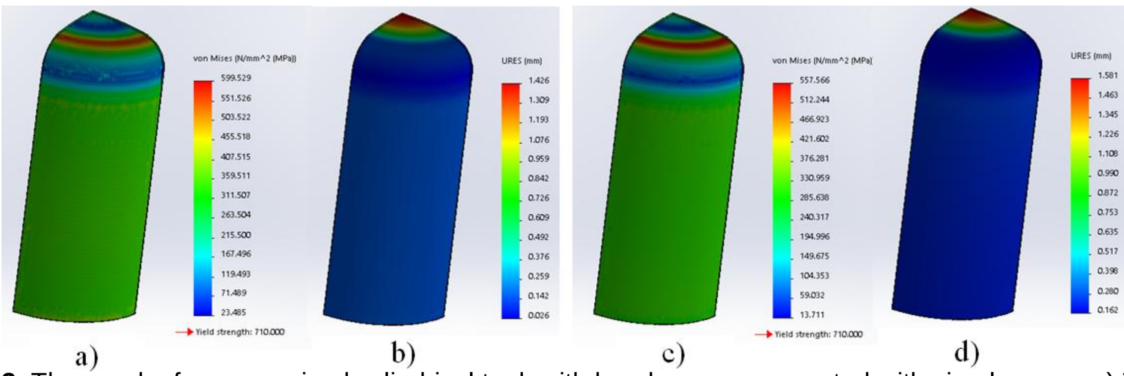

Fig. 23. The graphs for pressurized cylindrical tank with head covers connected with circular arcs: a) The Von Mises stress at T = -30 ^{0}C; b) The resultant linear deformation at T = -30 ^{0}C; c) The Von Mises stress at T = 60 ^{0}C; d) The resultant linear deformation at T = 60 ^{0}C

2.6. The optimized design of the cylindrical tank with flat head covers

The sketch and the parametric modeling of the flat head cover are shown in Figure 24.

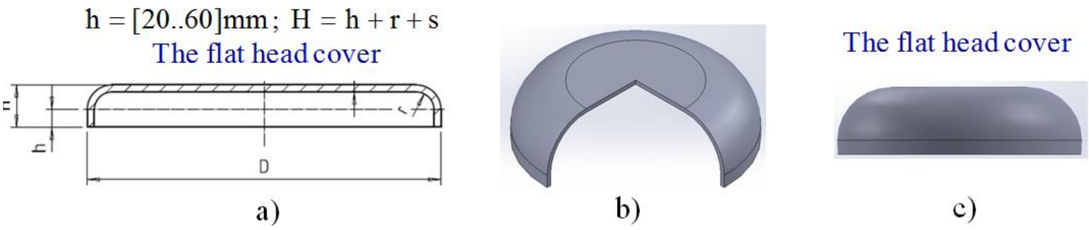

Fig. 24. a) The sketch of the flat head cover; b) The ¾ section of parametric model of the flat head cover; c) The front view of parametric model of the flat head cover

The variables subjected to optimization are: thickness s = 3…5 mm, the heights: h = 20...60 mm. and H = 30...70 mm. The obtained values are: s = 5 mm, h = 15 mm, H = 70 mm and radius r = 50 mm at T = -30 ^{0}C, with a maximum stress $\sigma_{rez.\ max}$ = 659.01 N/mm^2 and a linear resultant deformation u_{max} = 1.395 mm. The corresponding graphs of the stress and the state of the resulting linear deformation of the optimal cover head are shown in Figures 25a and 25b.

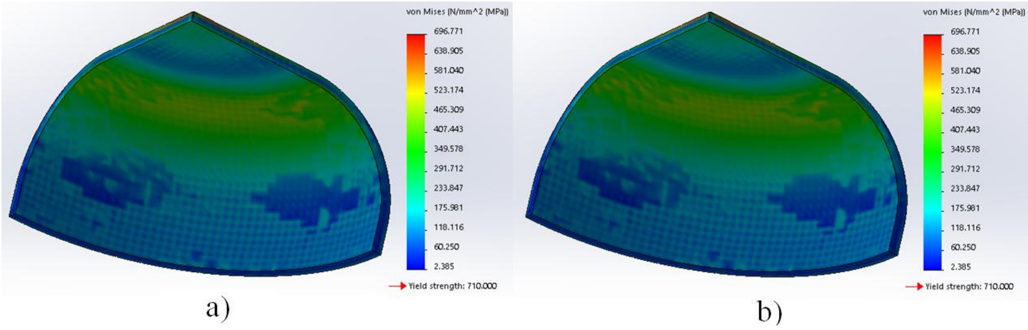

Fig. 25. The graphs for flat head cover a) The Von Mises stress; b) The resultant linear deformation

The minimum thickness of the flat cover is:

$$s_{real\ min} = 5 + 0.1\cdot 20 + abs(-0.6) + 0.1\cdot 8.5 = 8.45 \text{ mm} \tag{7}$$

A laminate sheet of AISI 4340 steel with a thickness of s = $8.5^{+0.25}_{-0.6}$ mm is chosen.
The graphs of stress and linear deformation of tank at T = -30 ^{0}C are shown in Figures 26a and 26b and for T = 60 ^{0}C in Figures 26c and 26d.

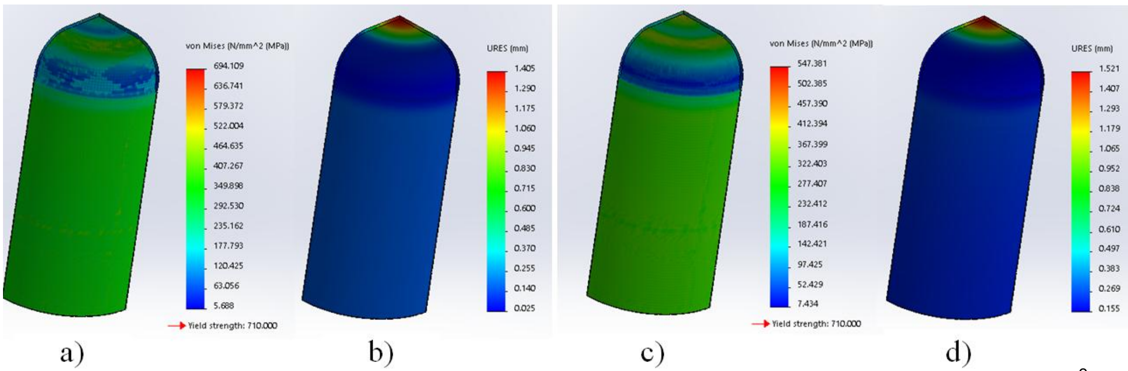

Fig. 26. The graphs for cylindrical tank with flat head covers: a) The Von Mises stress at T = -30 ^{0}C; b) The linear deformation at T = -30 ^{0}C; c) The Von Mises stress at T = 60 ^{0}C; b) The linear deformation at T = 60 ^{0}C

2.7. The optimized design of the cylindrical tank with back head covers connected with circular arcs

The sketch and the parametric model of the back head cover connected with circular arcs are shown in Figure 27.

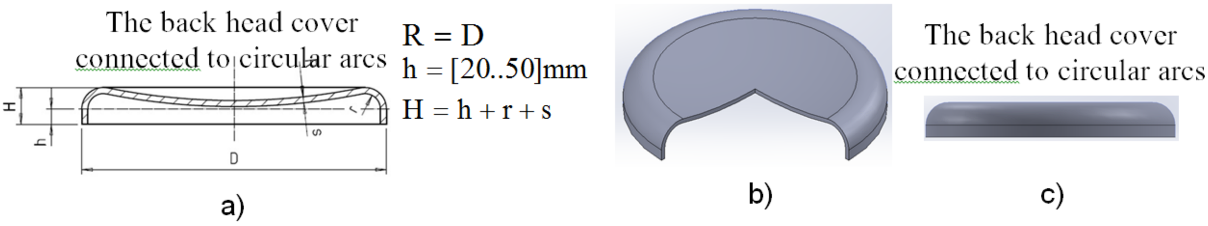

Fig. 27. a) The sketch of the back head cover connected with circular arcs; b) The ¾ section of parametric model of the back head cover connected with circular arcs; c) The front view of parametric model of the back head cover connected with circular arcs

The variables subjected to optimization are: s = 3...6 mm, h = 12...20 mm and H = 30...35 mm. The obtained values are: s = 4.5 mm, r = 22.5 mm, h =12 mm and H = 34.5 mm at T = -30 ^{0}C with a maximum stress $\sigma_{rez.\ max}$ = 628.27 N/mm^2 and a linear resultant deformation u_{max} = 1.873 mm.

The corresponding graphs of the stress and the state of the resulting linear deformation of the optimal back head cover are shown in Figures 28a and 28b.

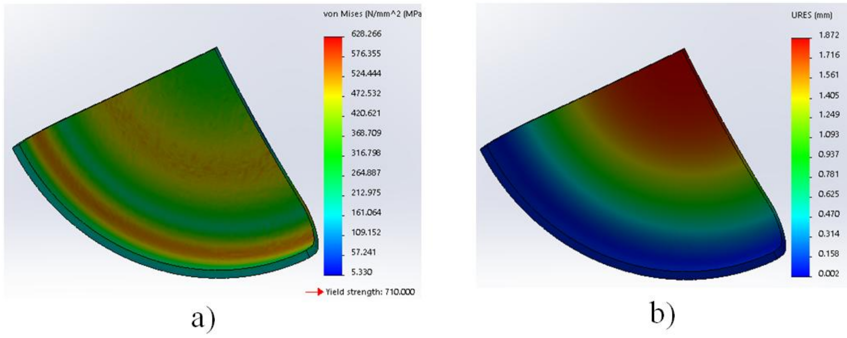

Fig. 28. The graphs for back head cover connected with circular arcs: a) The stress; b) The linear deformation

The minimum real thickness of the back head covers connected with circular arcs is:

$$s_{real\ min} = 4.5 + 0.1 \cdot 20 + abs(-0.6) + 0.1 \cdot 8 = 7.9 \text{ mm} \quad (8)$$

A laminate sheet of AISI 4340 steel with a thickness of $s = 8^{+0.25}_{-0.6}$ mm was chosen.
The corresponding graphs of the stress and the state of the resulting linear deformation of the tank at T = -30 ^{0}C are shown in Figures 29a and 29b and at T = 60 ^{0}C in Figures 29c and 29d.

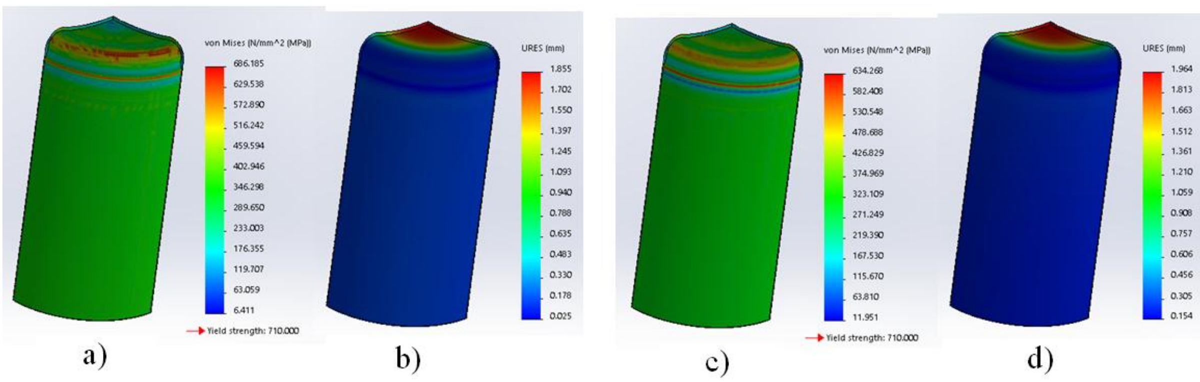

Fig. 29. The graphs for pressurized cylindrical tank with back head covers connected with circular arcs: a) The Von Mises stress at T = -30 ^{0}C; b) The resultant linear deformation at T = -30 ^{0}C; c) The Von Mises stress at T = 60 ^{0}C; b) The resultant linear deformation at T = 60 ^{0}C

The numerical values of state of stress and linear resultant deformation of the tanks are given in Table 1.

Table 1: The Von Misses stress and deformation of pressurized cylindrical tanks

		T= -30 ^{0}C		T= 60 ^{0}C	
No.	The type of pressurized cylindrical tank	σ [MPa]	u [mm]	σ [MPa]	u [mm]
1	Tank with torospheric head covers	658.312	0.604	592.657	0.695
2	Tank with ellipsoidal head covers	560.74	0.458	520.484	0.613
3	Tank with low pressure head covers	690.67	0.649	656.07	0.797
4	Tank with head covers connected with circular arcs	599.53	1.426	557.57	1.58
5	Tank with flat head covers	694.11	1.405	547.38	1.521
6	Tank with back head covers connected with circular arcs	686.185	1.855	634.268	1.964

The graphical representations of the Von Mises stress and the resulting linear deformation for T = -30 ^{0}C and T = 60 ^{0}C depending on the number's tank as specified in Table 1, computed for the end of the exploitation period (where n_a = 20 years) are shown in Figures 30 and 31.

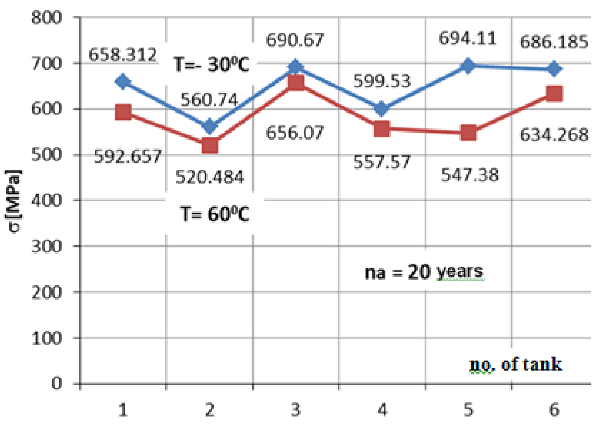

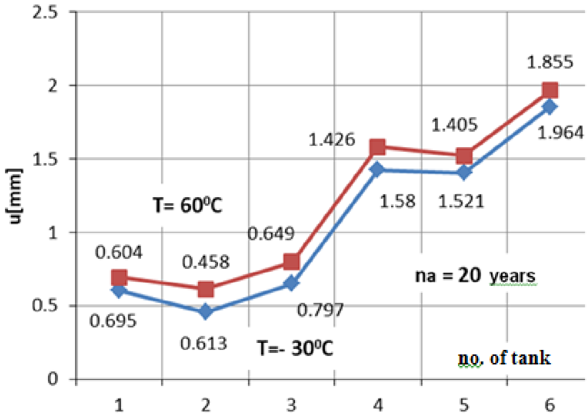

Fig. 30. The graphs for Von Mises stress at n_a = 20 years **Fig. 31.** The linear deformation at n_a = 20 years

In Figure 32 is shown the percentage variation of the Von Mises stress computed in respect to the admissible stress of material σ_a = 710 [MPa] at the temperatures of T = -30 ^{0}C and T = 60 ^{0}C, depending on the number of tank (as specified in Table 1) at n_a = 20 years of exploitation.

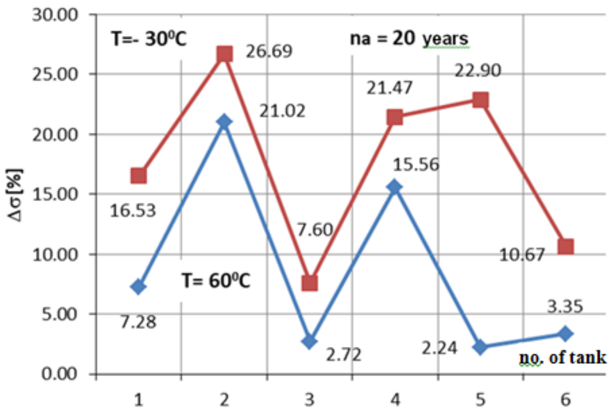

Fig. 32. The graphs for percentage variation of Von Mises stress at n_a = 20 years

3. Discussion

From these analyses shown in tables and graphical representations we can say that:

- The tank with ellipsoidal cover is the least loaded at both extreme temperatures, at T = -30 ^{0}C, σ_{max} = 560.74 MPa and T = 60 ^{0}C, σ_{max} = 520.48 MPa, according Figures 30 and 31.
- The flat cap tank has the highest stress value σ_{max} = 694.11 MPa at T = -30 ^{0}C and shows the greatest variation of stress between extreme temperatures, $\Delta\sigma$ = 146.73 MPa, according Figure 30.
- The tank with the low pressure head covers best accomplish for both extreme temperatures the conditions since the difference in admissible value is lower. It results that this tank is optimally dimensioned.
- The tank with head covers connected with circular arcs has the highest linear strain deformation u = 1.855 mm for T = 60 ^{0}C and the lowest value is found for the ellipsoidal head cover tank, as shown in Figure 31.
- The tank with low pressure head covers shows the minimum value of the percentage stress deviation $\Delta\sigma$ = 7.6 % at T = -30 ^{0}C and $\Delta\sigma$ = 2.72 % for T = 60 ^{0}C, that means it is the optimally dimensioned. At the opposite pole, the tank with ellipsoidal head covers has the greatest deviation of $\Delta\sigma$ = 26.69 % at T = -30 ^{0}C and $\Delta\sigma$ = 21.02 % for T = 60 ^{0}C, as shown in Figure 32.
- At the end of the exploitation period, the tank with the ellipsoidal head covers shows the largest reserve of resistance of stress $\Delta\sigma$ = 21.02 %, while the tank with flat head covers has the lowest resistance capacity $\Delta\sigma$ = 2.24 %, as shown in Figure 32.

4. Conclusions

According to the findings of the present study the following conclusions can be drawn:
- the Von Mises stress state and linear deformation of the tanks is directly influenced by: temperature variation, operating period, loading pressure and tank shape;
- at identical design input dates, for the end of the exploitation period, the tank with ellipsoidal head covers is the least subject to stress, followed in order by: tank with torospheric head covers, tank with low pressure head covers, tank with flat head covers and tank with back head covers connected with circular arcs which is subject to highest stress;
- the state of stress is lower at the maximum positive temperature than at the negative temperature for any type of tank, the stress variation curves for extreme operating temperature have about the same variation, except for this made the curve deviation at the tank with circular arcs;
- the resulting linear deformation is higher at the extreme positive and lower at the negative temperature for all tank types, and the order of increase the deformation is as follows: tank with ellipsoidal head caps, tank with low pressure head covers , tank with head covers connected with circular arcs, tank with flat head covers and the tank with back covers connected with circular arcs;
- from the point of view of stress and deformation, the tank with ellipsoidal head covers has the best shape and the most stressed is the tank with flat head covers;
- it is mentioned the fact that all the studied forms are optimized dimensionally in respect with the stress and deformation for which they were designed and work adequate.

Financial disclosure: Neither author has a financial or proprietary interest in any material or method mentioned.
Competing interests: The authors declare that they have no significant competing financial, professional or personal interests that might have influenced the performance or presentation of the work described in this manuscript.

References

[1] A.C. Nedelcu, "Romanian automotive industry – analysis made from the intellectual capital perspective", Revista Economica, vol. 67, no. 5, pp. 80-89, 2015;
[2] G. Matache, C. Cristescu, C. Dumitrescu, V. Miroiu, "Pregătirea specialiștilor în vederea adaptabilității și creșterii competitivității", Magazine of Hydraulics, Pneumatics, Tribology, Ecology, Sensorics, Mechatronics (HIDRAULICA), no. 3-4, pp. 7-14, 2012. ISSN 1453-7303;
[3] M. Rusănescu, "Material requirements planning, inventory control system in industry", Magazine of Hydraulics, Pneumatics, Tribology, Ecology, Sensorics, Mechatronics (HIDRAULICA), no. 1, pp. 21-25, 2014. ISSN 1453-7303;
[4] R. Khobragade, V. Hiwase, "Design, and analysis of pressure vessel with hemispherical and flat circular end", International Journal of Engineering Science and Computing, vol. 7, no. 5, pp. 12458-12469, 2017;
[5] D. H. Nash, "UK Rules for unfired pressure vessels". In: "The Companion guide to ASME boiler and pressure vessel code", 2008. ASME, Chapter 51. ISBN 9780971902717, https://strathprints.strath.ac.uk/6502;
[6] M.C. Ghiţă, A.C. Micu, M. Ţălu, Ş. Ţălu, "Shape optimization of vehicle's methane gas tank", Annals of Faculty of Engineering Hunedoara - International Journal of Engineering, Hunedoara, Tome X, Fascicule 3, pp. 259-266, 2012;
[7] M.C. Ghiţă, A.C. Micu, M. Ţălu, Ş. Ţălu, E. Adam, "Computer-Aided Design of a classical cylinder gas tank for the automotive industry", Annals of Faculty of Engineering Hunedoara - International Journal of Engineering, Hunedoara, Tome XI, Fascicule 4, pp. 59-64, 2013;
[8] M.C. Ghiţă, A.C. Micu, M. Ţălu, Ş. Ţălu, "3D modelling of a gas tank with reversed end up covers for automotive industry", Annals of Faculty of Engineering Hunedoara - International Journal of Engineering, Hunedoara, Tome XI, Fascicule 3, 2013, pp. 195-200, 2013;
[9] M.C. Ghiţă, A.C. Micu, M. Ţălu, Ş. Ţălu, "3D modelling of a shrink fitted concave ended cylindrical tank for automotive industry". Acta Technica Corviniensis – Bulletin of Engineering, Hunedoara, Romania, Tome VI, Fascicule 4, pp. 87-92, 2013;
[10] M.C. Ghiţă, A.C. Micu, M. Ţălu, Ş. Ţălu, Shape optimization of a thoroidal methane gas tank for automotive industry, Annals of Faculty of Engineering Hunedoara - International Journal of Engineering, Hunedoara, Tome X, Fascicule 3, pp. 295-297, 2012;

[11] M.C. Ghiţă, C.Ş. Ghiță, Ş. Ţălu, S. Rotaru, "Optimal design of cylindrical rings used for the shrinkage of vehicle tanks for compressed natural gas", Annals of Faculty of Engineering Hunedoara - International Journal of Engineering, Hunedoara, Tome XII, Fascicule 3, pp. 243-250, 2014;
[12] C. Bîrleanu, Ş. Ţălu, "Organe de maşini. Proiectare şi reprezentare grafică asistată de calculator" (Machine elements. Designing and computer assisted graphical representations), Cluj-Napoca, Victor Melenti Publishing house, 2001;
[13] Ș. Ţălu, "Limbajul de programare AutoLISP. Teorie şi aplicaţii", (AutoLISP programming language. Theory and applications), Cluj-Napoca, Risoprint Publishing house, 2001;
[14] Ş. Ţălu, "Reprezentări grafice asistate de calculator" (Computer assisted graphical representations), Cluj-Napoca, Osama Publishing house, 2001;
[15] Ş. Ţălu, "Grafică tehnică asistată de calculator" (Computer assisted technical graphics), Cluj-Napoca, Victor Melenti Publishing house, 2001;
[16] Ş. Ţălu, M. Ţălu, "A CAD study on generating of 2D supershapes in different coordinate systems", Annals of Faculty of Engineering Hunedoara - International Journal of Engineering, Hunedoara, Tome VIII, Fascicule 3, pp. 201-203, 2010;
[17] Ş. Ţălu, M. Ţălu, "CAD generating of 3D supershapes in different coordinate systems", Annals of Faculty of Engineering Hunedoara - International Journal of Engineering, Hunedoara, Tome VIII, Fascicule 3, pp. 215-219, 2010;
[18] Ş. Ţălu, "CAD representations of 3D shapes with superellipsoids and convex polyhedrons", Annals of Faculty of Engineering Hunedoara - International Journal of Engineering, Hunedoara, Tome IX, Fascicule 3, 2011, pp. 349-352, 2011;
[19] Ș. Ţălu, "AutoCAD 2005", Cluj-Napoca, Risoprint Publishing house, 2005;
[20] Ş. Ţălu, M. Ţălu, "AutoCAD 2006. Proiectare tridimensională" (AutoCAD 2006. Three-dimensional designing), Cluj-Napoca, MEGA Publishing house, 2007;
[21] Ş. Ţălu, "AutoCAD 2017", Cluj-Napoca, Napoca Star Publishing house, 2017;
[22] Ş. Ţălu, "Geometrie descriptivă" (Descriptive geometry), Cluj-Napoca, Risoprint Publishing house, 2010;
[23] A. Florescu-Gligore, M. Orban, Ş. Ţălu, "Cotarea în proiectarea constructivă şi tehnologică" (Dimensioning in technological and constructive engineering graphics), Cluj-Napoca, Lithography of The Technical University of Cluj-Napoca, 1998;
[24] A. Florescu-Gligore, Ş. Ţălu, D. Noveanu, "Reprezentarea şi vizualizarea formelor geometrice în desenul industrial" (Representation and visualization of geometric shapes in industrial drawing), Cluj-Napoca, U. T. Pres Publishing house, 2006;
[25] Ş. Ţălu, C. Racocea, "Reprezentări axonometrice cu aplicaţii în tehnică" (Axonometric representations with applications in technique), Cluj-Napoca, MEGA Publishing house, 2007;
[26] C. Racocea, Ş. Ţălu, "Reprezentarea formelor geometrice tehnice în axonometrie" (The axonometric representation of technical geometric shapes), Cluj-Napoca, Napoca Star Publishing house, 2011;
[27] T. Niţulescu, Ș. Ţălu, "Aplicaţii ale geometriei descriptive şi graficii asistate de calculator în desenul industrial" (Applications of descriptive geometry and computer aided design in engineering graphics), Cluj-Napoca, Risoprint Publishing house, 2001;
[28] Ş. Ţălu, "Micro and nanoscale characterization of three dimensional surfaces. Basics and applications", Napoca Star Publishing House, Cluj-Napoca, Romania, 2015;
[29] M. Țălu, "Calculul pierderilor de presiune distribuite în conducte hidraulice" (Calculation of distributed pressure loss in hydraulic pipelines), Craiova, Universitaria Publishing house, 2016;
[30] M. Țălu, "Pierderi de presiune hidraulică în conducte tehnice cu secțiune inelară. Calcul numeric și analiză C.F.D." (Hydraulic pressure loss in technical piping with annular section. Numerical calculation and C.F.D.), Craiova, Universitaria Publishing house, 2016;
[31] M. Ţălu, "Mecanica fluidelor. Curgeri laminare monodimensionale" (Fluid mechanics. The monodimensional laminar flow), Craiova, Universitaria Publishing house, 2016;
[32] M. Ţălu, "The influence of the corrosion and temperature on the Von Mises stress in the lateral cover of a pressurized fuel tank", Magazine of Hydraulics, Pneumatics, Tribology, Ecology, Sensorics, Mechatronics (HIDRAULICA), no. 4, pp. 89-97, 2017, ISSN 1453-7303;
[33] Ș. Ţălu, M. Ţălu, "The influence of deviation from circularity on the stress of a pressurized fuel cylindrical tank", Magazine of Hydraulics, Pneumatics, Tribology, Ecology, Sensorics, Mechatronics (HIDRAULICA), no. 4, pp. 34-45, 2017, ISSN 1453-7303;
[34] D. Vintilă, M. Ţălu, Ș. Ţălu, "The CAD analyses of a torospheric head cover of a pressurized cylindrical fuel tank after the crash test", Magazine of Hydraulics, Pneumatics, Tribology, Ecology, Sensorics, Mechatronics (HIDRAULICA), no. 4, pp. 57-66, 2017, ISSN 1453-7303;
[35] *** Autodesk AutoCAD 2017 software;
[36] *** SolidWorks 2017 software.